

PACS numbers: 42.55.Mv; 42.60.By
DOI: 10.1070/QE2001v031n06ABEH001989

Optimisation of a multistage pulsed dye laser system

S V Vasil'ev, M A Kuz'mina, V A Mishin

***Abstract*. A multistage narrow-band dye laser amplifying system with an output power of up to several kilowatts is considered as a whole. Such systems became necessary due to the development of the method of laser isotope separation (the AVLIS method). The use of the simplified model of an amplifying cell allowed us to solve analytically the equations describing the laser system and to determine optimal parameters of each stage. The dye laser system with an output power of 1 kW is optimised based on the model proposed. The accuracy of the obtained estimates was verified by a direct numerical simulation of the system based on a rigorous solution of the equations describing the interaction of radiation with the dye solution.**

Keywords: *laser isotope separation, dye laser*.

1. Introduction

At present, the solutions of organic dyes are the only active medium that can be used for the building of high-power tunable laser systems operating in the visible spectral range. The pumping of dye laser systems by copper vapour lasers provides several-kilowatt average output powers at a pulse repetition rate of tens of kilohertz and a pulse duration of tens of nanoseconds [1, 2].

The spectral parameters of a laser system are determined by a master oscillator, which often represents a single-frequency pulsed dye laser with the output power from several tens to hundreds of milliwatts. To achieve the required energy parameters of the laser system, the radiation from the master oscillator is amplified in several amplification stages.

The problem of optimisation of the laser system is formulated in the following way. Given the output power of the master oscillator, the output power of the laser system, the parameters of the pump laser and the dye type, it is necessary to provide the maximum laser efficiency, a simplicity and compactness of the laser system. Also, the number of amplifying cells and their parameters should be determined, as well as the pump power distribution over the cells.

S V Vasil'ev, M A Kuz'mina, V A Mishin General Physics Institute, Russian Academy of Sciences, ul. Vavilova 38, 119991 Moscow, Russia

Received 9 March 1999; revision received 15 November 1999
Kvantovaya Elektronika **31** (6) 505 – 509 (2001)
Translated by M N Sapozhnikov

2. Interaction of radiation with the dye solution and the model of an amplifying cell with the transverse pumping

The energy level diagram of a dye molecule is shown in Fig. 1. The energy spectrum of a dye consists of the system of singlet and triplet electronic levels. The vibration – rotation sublevels of each electronic state overlap with each other by forming broad bands, which provides the possibility of the laser frequency tuning. The radiative transitions in the dye occur between the sublevels of the lower singlet levels S_1 and S_0. The spontaneous decay of the S_1 level to the S_0 level occurs for several nanoseconds. The relaxation between the upper singlet and triplet levels within the electronic bands occurs nonradiatively for several picoseconds. The transitions between singlet and triplet electronic levels are forbidden in the dipole approximation and occur for several microseconds.

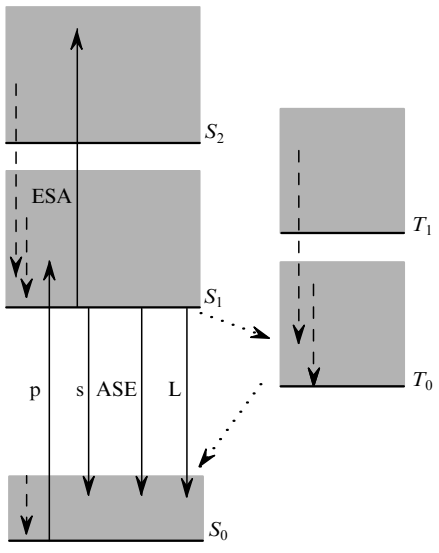

Figure 1. Energy level diagram of a dye molecule: S_m and T_n are singlet and triplet electronic levels. The solid arrows denote radiative transitions; the dashed arrows denote nonradiative relaxation; the dotted arrows denote the $S_m \leftrightarrow T_n$ transitions.

The scheme of the amplifying cell with transverse pumping is shown in Fig. 2. The active region represents a parallelepiped of size $a \times a \times A$ (hereafter, A is referred to as the length and a as the width of the active region). In the

dye solution, three types of photons are propagating: the pump radiation (subscript p), radiation being amplified (or laser radiation, subscript L), and spontaneous emission of the dye (subscript s). We assume that the propagation directions of laser radiation and spontaneous emission coincide with each other and with the x axis. The pump radiation is injected into the amplifier from two sides through side faces of the active region (along the y axis and in the opposite direction).

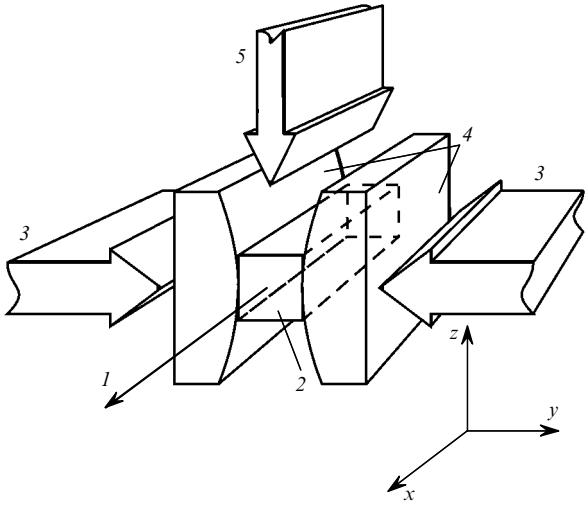

Figure 2. Scheme of a transversely pumped amplifying cell: (*1*) propagation direction of a beam being amplified; (*2*) active region of an amplifier; (*3*) pump beam; (*4*) windows of a dye cell; (*5*) dye flow.

By absorbing pump photons, dye molecules undergo transitions from the ground singlet S_0 state to the S_1 state and rapidly relax to the lower sublevels of the S_1 state. Then, the stimulated $S_1 \to S_0$ transition can occur accompanied by the creation of a photon at the laser wavelength (amplification), the spontaneous $S_1 \to S_0$ radiative transition, and the stimulated transition initiated by a spontaneous photon [amplified spontaneous emission (ASE)]. In addition, transitions between singlet and triplet levels are also possible. The main processes at which parasitic absorption of radiation occurs are the $S_1 \to S_2$ transitions (the ESA process [3, 4]) and the $T_0 \to T_1$ triplet transitions. The energy of photons absorbed in these processes is lost upon nonradiative relaxation.

Let a pulse being amplified have a duration about of ten nanoseconds and an average intensity of the order of 10^6 W cm^{-2}. Because the pulse duration is substantially shorter than the characteristic time of population of triplet levels, the influence of the $S \leftrightarrow T$ transitions can be neglected. For the radiation intensity under study, spontaneous radiative transitions occur for subnanoseconds, which is, on the one hand, substantially shorter than the pulse duration and, on the other, is longer than the nonradiative decay time. Therefore, we can use the quasi-stationary approximation in our calculations assuming that relaxation occurs instantly within each spectral band [5].

Based on the above model of the interaction of radiation with a dye, we write the kinetic equations for the level populations

$$\frac{\partial n_1}{\partial t} = \sigma_\mathrm{p} i_\mathrm{p} n_0 - \sigma_\mathrm{L} i_\mathrm{L} n_1 - \sigma_\mathrm{s} i_\mathrm{s} n_1 - \frac{n_1}{\tau} - \frac{n_1}{\tau_{ST}},$$

$$\frac{\partial n_T}{\partial t} = \frac{n_1}{\tau_{ST}} - \frac{n_T}{\tau_{TS}}, \quad n = n_1 + n_0 + n_T = \mathrm{const} \tag{1}$$

and the radiation transfer equations

$$\left(\frac{1}{c}\frac{\partial}{\partial t} \pm \frac{\partial}{\partial y}\right) i_\mathrm{p}^{\pm} = -\left(\sigma_\mathrm{p} n_0 + \sigma_\mathrm{p}^{(1)} n_1 + \sigma_\mathrm{p}^{(T)} n_T\right) i_\mathrm{p}^{\pm},$$

$$\left(\frac{1}{c}\frac{\partial}{\partial t} + \frac{\partial}{\partial x}\right) i_\mathrm{L} = \left[\left(\sigma_\mathrm{L} - \sigma_\mathrm{L}^{(1)}\right) n_1 - \sigma_\mathrm{L}^{(T)} n_T\right] i_\mathrm{L}, \tag{2}$$

$$\left(\frac{1}{c}\frac{\partial}{\partial t} \pm \frac{\partial}{\partial x}\right) i_\mathrm{s}^{\pm} = \left[\left(\sigma_\mathrm{s} - \sigma_\mathrm{s}^{(1)}\right) n_1 - \sigma_\mathrm{s}^{(T)} n_T\right] i_\mathrm{s}^{\pm} + \frac{\Omega}{4\pi}\frac{n_1}{\tau},$$

where n_0, n_1, and n_T are the populations of the levels S_0, S_1, and T_0; $i_{\mathrm{p,s}}^{\pm}$ are densities of pump and spontaneous photon fluxes (radiation intensities); superscripts $\pm$ correspond to the propagation directions along (+) the x axis and in the opposite direction (−); i_L is the laser radiation intensity; $i_\mathrm{p} = i_\mathrm{p}^{+} + i_\mathrm{p}^{-}$; $i_\mathrm{s} = i_\mathrm{s}^{+} + i_\mathrm{s}^{-}$; σ_β are cross sections for the stimulated $S_0 \leftrightarrow S_1$ transitions for photons of the type β ($\beta = \mathrm{p},\ \mathrm{s},\ \mathrm{L}$); $\sigma_\beta^{(1)}$ are cross sections for the $S_1 \leftrightarrow S_2$ transitions; $\sigma_\beta^{(T)}$ are the triplet absorption cross sections; τ is the spontaneous $S_1 \to S_0$ decay time; τ_{ST} and τ_{TS} are the characteristic times of transitions between singlet and triplet levels; c is the velocity of light in the dye solution; Ω is the solid angle in which spontaneous emission is amplified [6]. All the calculations were performed for Rhodamine 6G. We used the following values of kinetic constants: $\sigma_\mathrm{p} = 1.6 \times 10^{-16}$ cm^2, $\sigma_\mathrm{L} = \sigma_\mathrm{s} = 2.0 \times 10^{-16}$ cm^2, $\sigma_\beta^{(1)}/\sigma_\beta = 0.25$, $\tau = 3.5 \times 10^{-9}$ s [7].

To obtain qualitative estimates of the laser system parameters, we will pass on to the stationary approximation and neglect stimulated emission induced by a spontaneous photon. In this case, problem (1), (2) is reduced to the system of ordinary differential first-order equations

$$\frac{\mathrm{d}i_\mathrm{p}^{\pm}}{\mathrm{d}y} = \pm\left(\frac{\sigma_\mathrm{p}^{(1)} i_\mathrm{p} + \sigma_\mathrm{L} i_\mathrm{L} + 1/\tau}{\sigma_\mathrm{p} i_\mathrm{p} + \sigma_\mathrm{L} i_\mathrm{L} + 1/\tau}\right) \sigma_\mathrm{p} n i_\mathrm{p}^{\pm}, \tag{3a}$$

$$\frac{\mathrm{d}i_\mathrm{L}}{\mathrm{d}x} = n\frac{\sigma_\mathrm{p} i_\mathrm{p}\left(\sigma_\mathrm{L} - \sigma_\mathrm{L}^{(1)}\right) i_\mathrm{L}}{\sigma_\mathrm{p} i_\mathrm{p} + \sigma_\mathrm{L} i_\mathrm{L} + 1/\tau}. \tag{3b}$$

In amplifiers with the transverse pumping, the laser radiation intensity, as a rule, is substantially larger than the pump intensity, which allows us to replace the expression in the parentheses in equation (3a) by unity and to solve this equation analytically:

$$i_\mathrm{p}(y) = \frac{P_\mathrm{p}}{2aA}\left\{\exp\left[-\sigma_\mathrm{p} n\left(y + \frac{a}{2}\right)\right] + \exp\left[\sigma_\mathrm{p} n\left(y - \frac{a}{2}\right)\right]\right\}, \tag{4}$$

where P_p is the total pump power incident on the amplifying cell. We can easily find from (4) the fraction e of radiation absorbed by the active region, the average pump intensity $\bar{i}_\mathrm{p}$, and the depth of the dip (the inhomogeneity $\rho = i_\mathrm{p}^{\min}/i_\mathrm{p}^{\max}$ in the pump distribution over the cross section of the active region):

$$e = 1 - \exp(-\chi),\ \bar{i}_{\mathrm{p}} = \frac{P_{\mathrm{p}}}{aA}\frac{e}{\chi},$$
$$\rho = \frac{2}{\exp(\chi/2) + \exp(-\chi/2)}, \tag{5}$$

where

$$\chi = \sigma_{\mathrm{p}} n a. \tag{6}$$

Consider now equation (3b) for the radiation being amplified. Using relations (5), we replace the pump intensity i_{p} in (3b) by its average intensity $\bar{i}_{\mathrm{p}}$. To represent the solution of equation (3b) in a more clear form, we pass on from the radiation intensity to the efficiency η of the amplifying cell and the gain g in the cell:

$$\eta = \eta^{\max}(1 - \alpha k \ln g)\left(1 + \tilde{i}\frac{g \ln g}{g-1}\right)^{-1}. \tag{7}$$

Thus, the amplifying cell efficiency is determined by its gain g and four dimensionless coefficients α, $\tilde{i}$, $\eta^{\max}$ and k:

$$\eta = \frac{P_{\mathrm{L}}^{\mathrm{out}} - P_{\mathrm{L}}^{\mathrm{in}}}{P_{\mathrm{p}}}, \quad \alpha = \frac{a}{A}, \quad \eta^{\max} = e\left(1 - \frac{\sigma_{\mathrm{L}}^{(1)}}{\sigma_{\mathrm{L}}}\right),$$
$$g = \frac{P_{\mathrm{L}}^{\mathrm{out}}}{P_{\mathrm{L}}^{\mathrm{in}}}, \quad \tilde{i} = \frac{1}{\sigma_{\mathrm{L}}\tau}\left(\frac{P_{\mathrm{L}}^{\mathrm{out}}}{a^2}\right)^{-1}, \quad k = \frac{\sigma_{\mathrm{p}}}{\chi\left(\sigma_{\mathrm{L}} - \sigma_{\mathrm{L}}^{(1)}\right)}, \tag{8}$$

where $P_{\mathrm{L}}^{\mathrm{in}}$ and $P_{\mathrm{L}}^{\mathrm{out}}$ are powers of the laser radiation at the input and output of the cell. The coefficient α is the ratio of the transverse and longitudinal sizes of the amplifying cell. One can easily see from (7) that the amplifier efficiency increases with increasing the cell length A. The coefficient $\tilde{i}$ is the ratio of $1/\sigma_L\tau$ to the laser radiation intensity $P_{\mathrm{L}}^{\mathrm{out}}/a^2$ at the output from the active region. The amplifier efficiency also increases with decreasing $\tilde{i}$ (with increasing laser radiation intensity). The maximum efficiency of the amplifier (in the number of photons) is determined by the absorption coefficient for the pump radiation and by the ratio of the cross section for absorption from the excited state to the cross section for stimulated photoluminescence at the laser wavelength. If the length of the amplification region and the radiation intensity at the cell output are infinite, then

$$\lim_{\alpha,\tilde{i}\to 0} \eta = \eta^{\max}. \tag{9}$$

The coefficient k depends on the spectral parameters of the dye and the absorption coefficient for pump radiation. However, its influence on the amplifying cell efficiency is not substantial because it can be always compensated by changing the geometrical factor α.

Now, when the meaning of coefficients in expression (7) is clear, we determine the boundaries where they can vary. Fig. 3 shows the dependences of the fraction e of energy absorbed by the active region and of the inhomogeneity of the pump intensity distribution ρ on the parameter χ. One can see that absorption rapidly increases with increasing χ, resulting in the increase in the efficiency. However, the inhomogeneity of the pump intensity also increases. The main disadvantage of transverse pumping is that it cannot provide simultaneously the maximum use of the pump radiation and a high homogeneity of its distribution. In our opinion, the optimal value of χ lies within 2–3, which provides absorption of 85 %–95 % of the pump energy for an acceptable inhomogeneity $\rho \approx 0.5$. Below, we will always use the value $\chi = 2.5$.

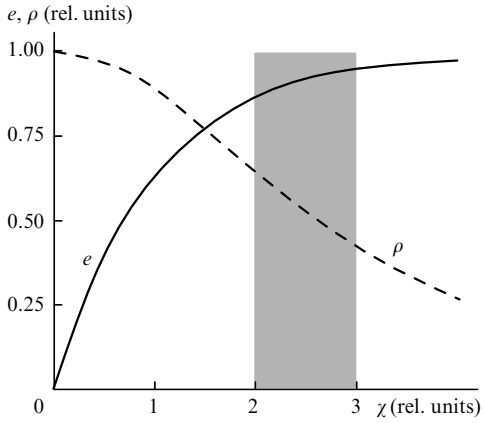

Figure 3. Absorption coefficient e for pump radiation and the inhomogeneity ρ of the pump intensity distribution over the cross section of an amplifying cell as functions of the parameter χ. The hatched region corresponds to optimal values of χ.

Another very important factor, which limits the amplifying cell efficiency, is the parameter $\tilde{i}$, which is determined by the limiting admissible radiation intensity. It is known, for example, that quartz withstands the radiation intensity up to 10^9 W cm^{-2}. However, this value is considerably lower at the solid state–dye solution interface due to the photo-induced dissociation of molecules of the active medium on the surface. Therefore, the limiting admissible radiation intensity depends on the types of a dye and solvent, as well as on the material of the amplifying cell windows, and can be determined only experimentally.

In paper [8], the value 20 MW cm^{-2} was used as the upper limit of the radiation intensity. However, the authors of paper [9] used the intensity 6 MW cm^{-2}. Possibly, this was related to the requirement to decrease the photodecomposition rate of the dye. The only free parameter in expression (7) within the framework of the approximations made above is the form factor α of the amplifying cell. However, it is clear that an increase in the cell length can result in losses caused by the diffraction divergence of a laser beam.

3. Optimisation of an amplifying system consisting of several cells

We will use our model of the transversely pumped amplifier to optimise a multistage amplifying system. The problem is formulated in the following way. At given laser radiation power $P_{\mathrm{L}}^{\mathrm{in}}$ incident on the amplifying system, the gain G, the number N of cells and the dye type, it is necessary to determine the geometrical parameters A_i and a_i, the dye concentration n_i, and the pump power $P_{\mathrm{p}\,i}$ for the ith cell of a stage which provide the maximum efficiency of the amplifying system. Since the amplifier efficiency is formally related to the pump power [(see Eqns (8)], we will determine the minimum pump power instead of the maximum efficiency because in this case the calculations are simplified.

Taking into account expressions (7) and (8), which were obtained for a single cell, we write the equations relating the parameters of the amplifying stage:

$$P_{\mathrm{p}\,i} = \frac{P_{\mathrm{L}\,i}}{\eta_i^{\max}} \frac{\tilde{i} g_i \ln g_i + g_i - 1}{1 - \alpha_i k_i \ln g_i}, \qquad (10)$$

$$P_{\mathrm{L}0} = P_{\mathrm{L}}^{\mathrm{in}},\ P_{\mathrm{L}\,i+1} = g_i P_{\mathrm{L}\,i},\ G = g_0 g_1 \ldots g_N.$$

The choice of the relation between the dye concentration and the transverse size of amplifying cells at which the distributions of the pump intensity are identical at all the stages is quite reasonable from a practical point of view. It follows from this condition and relations (5), (6), and (8) that parameters $\eta_i^{\max}$ and k_i should coincide for all the cells.

The limiting admissible radiation intensity is one of the critical parameters of the amplifying system. To provide the same radiation load on all the stages of the amplifying system, we require that the maximum intensities $L_{\mathrm{L}\,i}^{\max}$ of laser radiation at the output of each cell would be the same, meaning the equality of parameters $\tilde{i}_i$. Analysis of an individual amplifying stage showed that, if the amplification of spontaneous emission and diffraction effects are neglected, the cell efficiency increases monotonically with its length. In the study of the multistage amplifier, we will choose the lengths of cells so that their efficiencies would differ from the maximum efficiency (for given amplification and intensity) by the same coefficient ξ (below, we will use the value $\xi = 0.9$).

The above conditions allow us to relate the dye concentration and the cell size with the gain of cells:

$$\chi_i = \sigma_{\mathrm{p}} n_i a_i = \chi = \mathrm{const}, \qquad (11a)$$

$$i_{\mathrm{L}\,i}^{\max} = g_0 g_1 \ldots g_i \frac{P_{\mathrm{L}0}}{a_i^2} = i_{\mathrm{L}}^{\max} = \mathrm{const}, \qquad (11b)$$

$$\xi_i = 1 - \alpha_i k_i \ln g_i = \xi = \mathrm{const}. \qquad (11c)$$

It follows from (11a), (11b), and (11c), respectively, that $\eta_i^{\max} = \eta^{\max} = \mathrm{const}$ and $k_i = k = \mathrm{const}$; $\tilde{i}_i = \tilde{i} = \mathrm{const}$; $\alpha_i = (1-\xi)/k \ln g_i$. Taking this into account, the substitution of (11) into (10) gives

$$P_{\mathrm{p}\,i} = \frac{P_{\mathrm{L}0}}{\xi \eta^{\max}} g_0 \ldots g_{i-1} \left(\tilde{i} g_i \ln g_i + g_i - 1\right), \qquad (12)$$

$$G = g_0 g_1 \ldots g_N.$$

Thus, only a set of the cell gains g_i remains unknown. By determining these gains, we can calculate the other parameters of the multistage amplifier.

A multistage amplifier is most often optimised using the condition of the uniform distribution of the gain over the cells:

$$g_0 = g_1 = \ldots = g_N = G^{1/(N+1)}. \qquad (13)$$

In this case, the amplification in each cell occurs in the same way and the cells have equal efficiencies, which coincide with the efficiency of the multistage amplifier as a whole. This means that criterion (13) allows one to estimate the parameters of the amplifier by analysing one amplifying cell [in our case, by using relations (7) and (8)]. Such an approach (hereafter, referred to as a standard method) is intuitively clear and allows an easy scaling of the amplifier.

To verify whether a standard method of division of the multistage amplifier into individual cells is also the best from the point of view of the amplifier efficiency, we perform the formal mathematical study of the multistage amplifier. From (12), we obtain the expression for the total pump power of the $(N+1)$-stage amplifying system:

$$P_{\mathrm{p}}^{\mathrm{tot}} = P_{\mathrm{L}0} \frac{\tilde{i}}{\xi \eta^{\max}} \left[\frac{G-1}{\tilde{i}} + G \ln G + (g_0 - G) \ln g_0 \right.$$

$$\left. + (g_0 g_1 - G) \ln g_1 + \ldots + (g_0 \ldots g_{N-1} - G) \ln g_{N-1} \right]. \qquad (14)$$

We will consider $P_{\mathrm{p}}^{\mathrm{tot}}$ as a function of N variables $g_0, g_1, \ldots, g_{n-1}$. It is known that the necessary condition for the existence of an extremum of a function is the vanishing of all its first partial derivatives. By setting these derivatives to zero and making simple transformations, we obtain the system of equations to which the gains of cells in the most efficient amplifier should satisfy:

$$\begin{aligned} g_1 &= \ln g_0 + 1, \\ g_2 &= \ln g_1 + 1, \\ &\ldots\ldots\ldots\ldots \\ g_N &= \ln g_{N-1} + 1, \\ G &= g_0 g_1 \ldots g_N. \end{aligned} \qquad (15)$$

Fig. 4 shows the distribution of the gain over the stages for the optimised and standard amplifying systems with the gain $G = 10^4$. The dependences were plotted for the 2-, 3-, 4-, and 5-stage amplifiers. One can easily see that the gain in the optimised system is distributed over cells quite nonuniformly. The gain in the first cell in the optimised system is always substantially greater than that in the standard system, whereas the gains in the subsequent cells in the former case are smaller. Therefore, the first cell in the optimised system operates in the 'overpumped' regime with a comparatively low efficiency, whereas the rest of the cells operate in the saturated regime with a high efficiency.

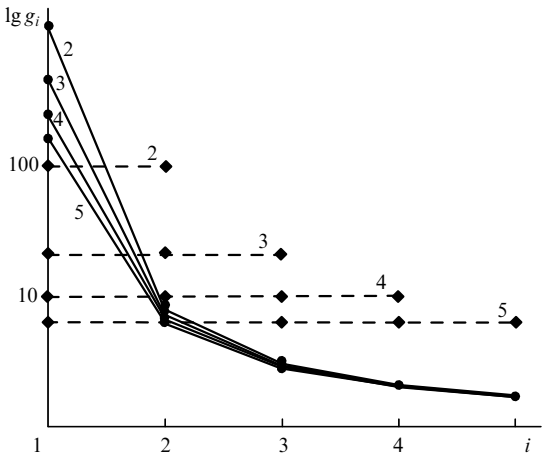

Figure 4. Distribution of the gain over amplifying cells for the optimised (solid curves) and standard (dashed curves) systems; the numbers at the curves are a total number of cells in the amplifying system.

Consider now the influence of the system optimisation on its total efficiency and length, which are the most important parameters of the system from the practical point of view. Fig. 5 shows the dependences of these parameters on the number of stages for the amplifier with an average input power of 100 mW (the pulse duration was 10 ns and the pulse repetition rate was 10 kHz), the gain $G = 10^4$, and the maximum radiation intensity $i_L^{max} = 10$ MW cm^{-2}. One can see that the optimised multistage system offers a noticeable advantage both in the efficiency and in the compactness of the amplifying system, which allows one either to reduce the number of cells, without decreasing the efficiency, or to increase the efficiency without adding new cells.

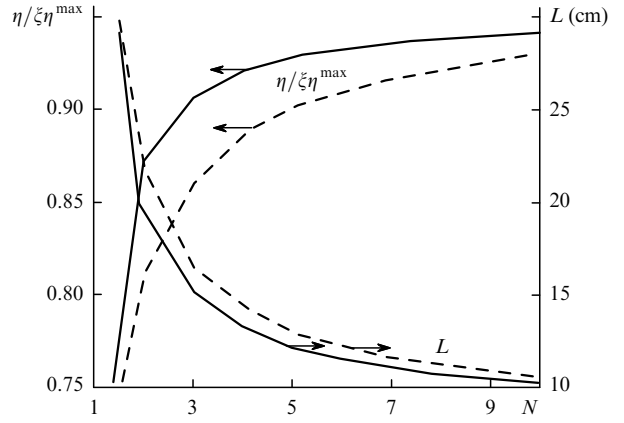

Figure 5. Efficiency $\eta/\xi\eta^{max}$ and length L of an amplifying system as functions of the number N of cells for the optimised (solid curves) and standard (dashed curves) systems.

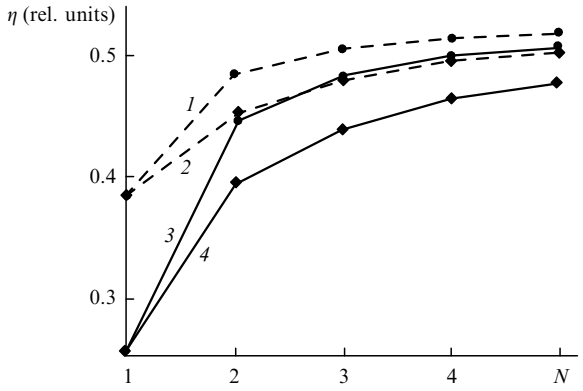

Figure 6. Efficiency η of the amplifying system as a function of the number N of cells for the simplified model (*1*, *2*) and rigorous numerical calculation (*3*, *4*) for the optimal (*1*, *3*) and standard (*2*, *4*) divisions of the system into cells.

To estimate the accuracy with which our simplified model describes the amplifying system, we compared the analytic estimates obtained above with the results of rigorous numerical simulations. The exact results were obtained by directly solving equations (1) and (2), i.e., we solved a nonstationary problem by taking into account triplet absorption and ASE. In addition, we considered the distribution of particles over the sublevels within electronic bands.

We determined the parameters of the amplifiers using both standard (13) and optimal (15) criteria for the division of the amplifying system into cells. The dependences of the multistage system efficiency on the number of stages are shown in Fig. 6. We used in calculations the same system parameters as in Fig. 5. As expected, the ideal model of an amplifying cell gives the overestimated values, however, the types of the approximated and exact dependences are similar. Moreover, the rigorous mathematical model more distinctly demonstrates the advantages of the method proposed for the system optimisation.

4. Conclusions

The method proposed for optimisation of transversely pumped multistage dye amplifying systems showed that the optimisation of the pump intensity distribution between the stages substantially improves the parameters of the amplifying system. The analytic expressions obtained in the paper allow one to calculate the parameters of amplifying cells used in the systems. Comparison of the results of the theoretical study with rigorous numerical calculations confirms the correctness of the approximations used.

Acknowledgements. The authors thank researchers of the Laboratory of Atomic Spectroscopy, General Physics Institute, RAS, for useful discussions and support of this study.

References

1. Mishin V A *Trudy II Vserossiiskoi Konferentsii 'Fiziko-Khimicheskie Protsessy pri Selektsii Atomov i Molekul'* (Proceeding of II All-Russian Conference on Physicochemical Processes upon Selection of Atoms and Molecules) (Zvenigorod, 1997), p. 12 – 20
2. Batenin V M, Buchanov V V, Kazaryan M A, Klimovskikh I I, Molodykh E I *Lazery na Samoogranichennykh Perekhodakh Atomov Metallov* (Metal Atom Self-Terminating Lasers) (Moscow: Nauchnaya Kniga, 1998)
3. Sahar E, Treves D *IEEE J. Quantum Electron.* **13** 962 (1977)
4. Dasgupta K, Nair L G *IEEE J. Quantum Electron.* **26** 189 (1990)
5. Hargrove R S, Kan T *IEEE J. Quantum Electron.* **16** 1108 (1980)
6. Haag G, Munz M, Marowsky G *IEEE J. Quantum Electron.* **19** 1149 (1983)
7. Sugiyama A, Nakayama T, Kato M, Maruyama Y *Appl. Opt.* **36** 5849 (1997)
8. Duarte F J, Ed. *High-Power Dye Lasers* (Springer Series in Optical Sciences) (Berlin: Springer-Verlag, 1991) vol. 65
9. Takehisa K *Appl. Opt.* **36** 584 (1997)